In situ measurements of gas/particle-phase transitions for atmospheric semivolatile organic compounds

Brent J. Williams[a,b,c,1], Allen H. Goldstein[a,d], Nathan M. Kreisberg[e], and Susanne V. Hering[e]

[a]Department of Environmental Science, Policy, and Management, University of California, 147 Mulford Hall, Berkeley, CA 94720; [b]Aerodyne Research Inc., 45 Manning Road, Billerica, MA 01821; [c]Department of Mechanical Engineering, University of Minnesota, 271 Mechanical Engineering, 111 Church Street S.E., Minneapolis, MN 55455; [d]Department of Civil and Environmental Engineering, University of California, 147 Mulford Hall, Berkeley, CA 94720; and [e]Aerosol Dynamics Inc., 935 Grayson Street, Berkeley, CA 94710

Edited by Barbara J. Finlayson-Pitts, University of California, Irvine, CA, and approved December 15, 2009 (received for review October 13, 2009)

An understanding of the gas/particle-phase partitioning of semivolatile compounds is critical in determining atmospheric aerosol formation processes and growth rates, which in turn affect global climate and human health. The Study of Organic Aerosol at Riverside 2005 campaign was performed to gain a better understanding of the factors responsible for aerosol formation and growth in Riverside, CA, a region with high concentrations of secondary organic aerosol formed through the phase transfer of low-volatility reaction products from the oxidation of precursor gases. We explore the ability of the thermal desorption aerosol gas chromatograph (TAG) to measure gas-to-particle-phase transitioning for several organic compound classes (polar and nonpolar) found in the ambient Riverside atmosphere by using in situ observations of several hundred semivolatile organic compounds. Here we compare TAG measurements to modeled partitioning of select semivolatile organic compounds. Although TAG was not designed to quantify the vapor phase of semivolatile organics, TAG measurements do distinguish when specific compounds are dominantly in the vapor phase, are dominantly in the particle phase, or have both phases present. Because the TAG data are both speciated and time-resolved, this distinction is sufficient to see the transition from vapor to particle phase as a function of carbon number and compound class. Laboratory studies typically measure the phase partitioning of semivolatile organic compounds by using pure compounds or simple mixtures, whereas hourly TAG phase partitioning measurements can be made in the complex mixture of thousands of polar/nonpolar and organic/inorganic compounds found in the atmosphere.

gas chromatography | mass spectrometry | organic aerosol | phase partitioning | thermal desorption

Atmospheric particles are detrimental to human health (1–4) and influence our global energy balance (5) and hydrological cycle (6, 7). The carbonaceous component of ambient particles makes up a large fraction of the total fine-particle mass, typically 20–80% (8), and is key in determining particle sources and transformation processes. Atmospheric organic aerosol (OA) budgets are still highly uncertain, largely because we do not understand the fate of gas-phase volatile organic compounds (VOCs) (6, 9). A majority of the organic material in the atmosphere is in the gas phase (10). Gas-phase compounds with lower vapor pressures can partition to the particle phase; additionally, as gas-phase compounds undergo photooxidation in the atmosphere, the resulting reaction products can display lower vapor pressures that allow them to partition into the particle phase, forming secondary organic aerosol (SOA) (11). SOA was found to contribute an average of ~75% of summertime total fine OA mass in Riverside, CA (12).

Most observations of particle-phase organics treat adsorption from the gas phase as an artifact, ignoring or removing the data impacted by gas/particle-phase partitioning (6). With a thermal desorption aerosol gas chromatograph (TAG), we discovered that the gas-phase adsorption in the collection cell contains critical information on in situ gas/particle transitioning as a function of molecular size and functionality for semivolatile organic compounds in the atmosphere, a need that has been specifically called for by the atmospheric research community (13). In this paper, we use field observations to define phase transition points and compare the gas- and particle-phase TAG observations to partitioning theory.

Measurement Site

Data presented here were collected as part of the Study of Organic Aerosol at Riverside (SOAR) during the summer and fall of 2005 at the University of California, Riverside. Throughout this paper, data reported as averages were averaged over an 11-day focus period in the summer (July 29–August 8) and an 11-day focus period in the fall (November 4–14). Data included in this paper were principally collected on a TAG (14). Total $PM_{2.5}$ (particulate matter with diameters <2.5 μm) mass concentration was measured by a beta attenuation monitor (BAM) at the California Air Resources Board monitoring station at Rubidoux, CA, located 10 km northwest of the SOAR site. At the SOAR site, nonrefractory $PM_{1.0}$ mass concentration, with a separation between organics, SO_4^{2-}, NO_3^-, NH_4^+, and chloride, was measured by an Aerodyne high resolution time-of-flight aerosol mass spectrometer (AMS) (12, 15). Elemental carbon (EC) was measured by using an EC/OC monitor (Sunset Labs) (16). VOCs were measured by using a VOC gas chromatograph/mass spectrometer (GC/MS) (17). A full suite of meteorological parameters were also measured, including photosynthetically active radiation (PAR), which serves as an indication of sunlight. All measurements have been averaged onto the same timeline as hourly TAG measurements, only incorporating data from the half hour in which TAG was sampling.

Hourly, Speciated Organic Aerosol Measurements

Briefly described, TAG is an in situ instrument to identify and quantify OA chemical composition with 1-hour time resolution, a significant improvement over typical 12- to 24-hour filter-based collection with subsequent laboratory analysis. Atmospheric particles are collected by humidification and inertial impaction. The sample is then thermally desorbed onto a GC column for compound separation with subsequent detection by quadrupole mass spectrometry. With the exception of periodic manually applied liquid calibration standards, TAG is fully automated, offering continuous measurements to determine diurnal, weekly, and seasonal patterns in OA composition (14).

Automated TAG sampling was set on a 26-hour cycle throughout the study, including 19 ambient aerosol collections, 5 filtered

Author contributions: B.J.W., A.H.G., N.M.K., and S.V.H. designed research; B.J.W. and N.M.K. performed research; B.J.W. and N.M.K. analyzed data; and B.J.W., A.H.G., N.M.K., and S.V.H. wrote the paper.

The authors declare no conflict of interest.

This article is a PNAS Direct Submission.

[1]To whom correspondence should be addressed. E-mail: brentw@me.umn.edu.

This article contains supporting information online at www.pnas.org/cgi/content/full/0911858107/DCSupplemental.

www.pnas.org/cgi/doi/10.1073/pnas.0911858107

ambient samples, 1 zero air sample (AADCO 737, zero air generator, Cleves, OH), and 1 filtered zero air sample. Filtered samples were obtained by sending the sample stream through a Teflon membrane filter (Zefluor 2.0 μm, Pall Corp.) prior to humidification. These filtered ambient samples were used to detect any collection of gas-phase compounds. It is likely that gas-phase collection occurs both at the inertial-impaction site and on the collection cell walls. Zero air samples were used to test for within-system contamination (i.e., zero air sample) and for desorption from the filter (i.e., filtered zero air sample). Zero air and filtered zero air collections had near-zero abundance for all integrated compounds.

Because large quantities of H_2O can interfere with chromatographic separation and saturate the ion source and detector, a brief 50 °C temperature soak was used to purge H_2O from the sample before injection onto the column. This temperature soak was applied to both ambient and filtered ambient collections during both seasons and potentially alters the observed phase transitioning from ambient phase transitioning, a point further evaluated later in this paper. Active humidification was not applied for summertime sampling due to elevated relative humidity (R.H.) caused by drawing warm ambient air into a cooler sampling container. Average summertime sampling R.H. was ~60%. Active humidification was applied during the fall, and average sampling R.H. was ~70%.

Particle-phase calibrations are performed by using syringe injections of known quantities of liquid standards. A wide range of polar and nonpolar compounds were periodically injected. No gas-phase calibration standards were analyzed on the TAG system during the study; thus, gas-phase collection was not quantified. However, it is still of interest to explore what can be learned from the portion of the gas phase that was collected.

Ambient measurements are the combination of the particle phase and adsorbed vapors, whereas the Teflon filter measurement provides a measure of the adsorbed vapor. Therefore the particle value is calculated as the difference between these two measurements. To compare gas-phase and particle-phase values, we must interpolate the separate sampling periods onto the same timeline. For analyses that involve taking an average of all data (e.g., average phase partitioning), the lower time-resolution gas-phase timeline has been used to maintain the accuracy of ambient concentration variability.

Observable Semivolatile Compounds

Just less than 300 semivolatile organic compounds were identified in TAG chromatograms during the SOAR study. These compounds represent a wide range of chemical classes, including nonpolar hydrocarbons such as n-alkanes, alkenes, and polycyclic aromatic hydrocarbons (PAHs), to polar oxygenated classes such as acids, ketones, and aldehydes. These compounds also represent a wide range of molecular sizes, with molecular weights ranging from 98 to 436 g mol^{-1}, with an average of 220 g mol^{-1}, calculated with equivalent influence from each observed compound.

For the purpose of determining TAG's ability to observe semivolatile compounds that are actively partitioning between physical states, it is of interest to determine the range of observable volatility and polarity by using this technique. Fig. 1 shows the gas chromatographic retention time (*x* axis) and oxygen:carbon (O:C) ratio (primary *y* axis) for the nearly 300 compounds observed and identified during SOAR. The retention time roughly divides compounds by volatility, with highly volatile compounds at early retention times and nonvolatile compounds at late retention times. The O:C ratio roughly divides compounds by polarity, with nonpolar compounds at zero on the *y*-axis scale and the most polar compounds over 0.5 on the *y*-axis scale. Many of the compounds fall into specific patterns on the basis of their oxygen and carbon content. Contours of varying oxygen and carbon content have been outlined. The observable O:C ratio is limited by the chromatography column, which does not allow efficient transfer of many multifunctional oxygenated compounds. This range could be extended with chemical derivatization (18). Observable low-volatility compounds are limited by the top thermal desorption and GC oven temperatures. This range could be extended with components rated to higher temperatures (e.g., chromatography columns, ferrules, transfer lines). Observable high-volatility compounds are limited by collection technique. This range could be extended by including a more complete gas-phase collection method. A complete list of compounds included in Fig. 1 can be found in Table S1.

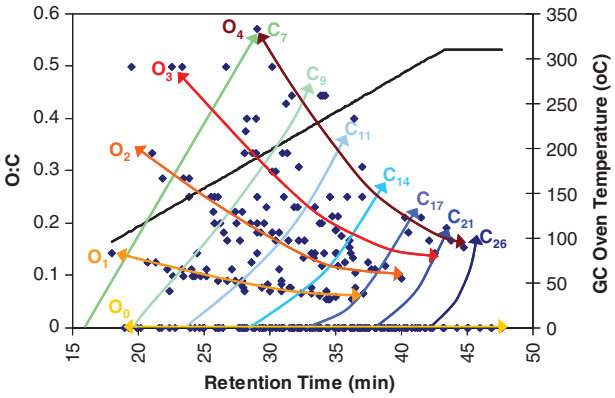

Fig. 1. Molecular size and polarity window for approximately 300 identified compounds measured by TAG. Compound retention time from GC shown in minutes on the *x* axis. The primary *y* axis shows the oxygen (O) to carbon (C) ratio. The secondary *y* axis relates retention time to oven temps, shown as a black line.

As will be shown below, compounds with the earliest retention times are almost fully in the gas phase, and compounds with the latest retention times are almost fully in the particle phase. TAG appears to include the critical window of semivolatile compounds, a measurement window that is often ignored in gas-phase studies and particle-phase studies because of interference between the two physical states. This semivolatile organic compound window is roughly defined by vapor pressures ranging between 10^{-2} and 10^{-8} Torr (9).

Many compounds found in this volatility range are lower-volatility photooxidation products of VOCs. The photooxidation of naphthalene, a PAH, serves as a good example of a gas-phase compound that reacts in the atmosphere to form lower-volatility reaction products. A major reaction product of naphthalene and the OH radical is phthalic anhydride, which is believed to quickly undergo hydrolysis once in the particle phase to form phthalic acid (19). Phthalic acid is found in high concentrations in the atmosphere and has been suggested as a single-species surrogate for the contribution of SOA to ambient aerosol (20), making it an important marker compound for aerosol source apportionment purposes. At 25 °C, naphthalene has a vapor pressure of 8.5×10^{-2} Torr, whereas phthalic acid has a lower vapor pressure of 6.4×10^{-7} Torr (21).

Ambient relative abundance timelines of gas-phase plus particle-phase naphthalene and phthalic acid as measured by TAG during the summer SOAR study are shown in Fig. 2*A*, along with PAR, which is a measure of daylight. Because the gas-phase portion of these compounds is not quantified, relative abundance timelines are used to show the mixed-phase signal instead of mass concentrations. Fig. 2*B* displays these compounds' relative abundances fit to an average diurnal cycle. According to TAG collection, these two compounds are anticorrelated ($r = -0.7$). Naphthalene concentrations are likely decreased during the daytime as a result of increased dilution and oxidation, and phthalic acid concentrations are likely increased during the daytime as a result of secondary production in the atmosphere.

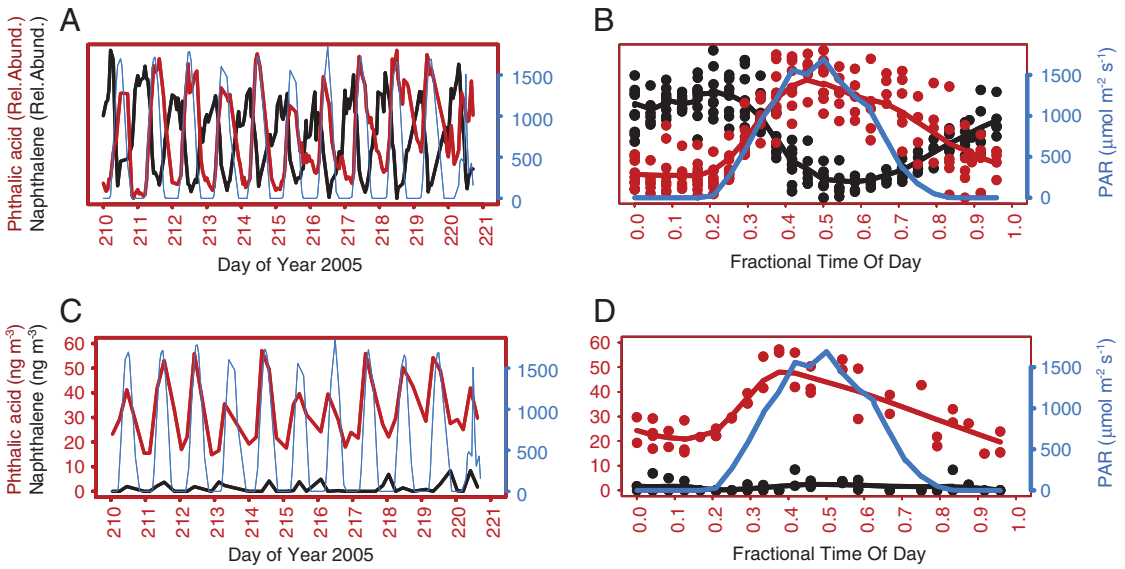

Fig. 2. Summertime observations of naphthalene and its oxidation product phthalic acid at Riverside, CA. (*A*) Anticorrelated relative abundance timelines for gas + particle-phase naphthalene and phthalic acid. PAR displays sunlight patterns. (*B*) Diurnal cycles, again showing anticorrelation and phthalic acid increasing with PAR. (*C*) Particle-phase mass concentrations for naphthalene and phthalic acid. Little naphthalene enters the particle phase, where phthalic acid has high concentrations in the particle phase. (*D*) Diurnal cycles of particle-phase concentrations.

Fig. 2*C* and *D* is similar to the previous figures but now includes only the quantified particle-phase mass concentrations. Here, it is clear that very little naphthalene enters the particle phase (i.e., on average, 1.4 ± 2.3 ng m^{-3} in summer, 4.4 ± 5.9 ng m^{-3} in fall), but the reaction product, phthalic acid, is able to more efficiently enter the particle phase (i.e., on average, 32.2 ± 12.7 ng m^{-3} in summer, 30.9 ± 12.8 ng m^{-3} in fall). This trend is expected for many gas-phase compounds undergoing oxidation in the atmosphere, creating lower-volatility reaction products and forming SOA. The quantity of naphthalene observed in the particle phase here is similar to the annual average observed previously at Riverside (6.72 ± 11.6 ng m^{-3}), where naphthalene was found to be approximately 1% in the particle phase and 99% in the gas phase (22).

The collected gas phase made up 100% of the most volatile compounds' abundance, as compared to an ambient run (i.e., gas-phase and particle-phase signal). There was no direct overlap between species measured on the VOC GC/MS and the TAG system. However, both the VOC GC/MS and the TAG system detected monoterpenes. A clear correlation is found between limonene measured by TAG and monoterpenes measured by VOC GC/MS ($r = 0.72$ with α-pinene, $r = 0.84$ with β-pinene). Approximately 20% of the signal from limonene is in the particle phase according to TAG sampling. The variability in atmospheric concentrations of gas-phase species appears to be captured reasonably well by TAG, but it is expected that only a fraction of the total gas-phase mass is collected because the vapor pressure of limonene is approximately 1.5 Torr (21) and would be expected to be less than 1% in the particle phase. Timelines of α-pinene and β-pinene as measured by VOC GC/MS and limonene as measured by the TAG system are shown in Fig. S1.

Phase Transitioning by Compound Class and Molecular Size

To further explore what can be learned from TAG measurements of semivolatile compounds, we will take a closer look at TAG-observed phase partitioning of specific compound classes and for a wide range of molecular sizes. We will then compare the observed partitioning to modeled partitioning for a subset of compound classes.

Fig. 3 explores the phase transitioning trends of semivolatile compounds as observed by TAG. Here, compounds are grouped by compound class and sorted by the number of carbon atoms within the molecule across the *x* axis. Compounds are plotted on the basis of the average fraction of their total relative abundance that is found in the particle phase and averaged separately across each season. If a compound is 100% particle phase, then its *y*-axis value will be 1. A compound that is fully in the gas phase will have a value of 0. The average summer (fall) temperature was 26 °C (16 °C). Specific compounds used in the analysis are shown in bold font in Table S1. Several partitioning points are the average of multiple compounds with the same functional groups and carbon number.

The smallest alkanes are almost entirely in the gas phase, and the particle-phase portion increases with increasing carbon number. Upon reaching the C_{27} alkane (heptacosane), the alkanes become fully particle phase. For other compound classes, molecules with smaller carbon numbers transition into the particle phase because of decreased vapor pressure with increased functionality and polarity.

There are seasonal differences in phase transition points. Each compound is shifted toward higher particle-phase fractions during the fall. Organic semivolatile compounds can more easily enter the particle phase if there is more ambient OA particle mass; however, whereas total particle mass concentrations were higher in the fall, organic mass concentrations were very similar during both seasons (Table 1). Therefore, this slight seasonal phase shift is likely due in part to the cooler fall atmospheric temperatures driving semivolatile compounds into the particle phase. Even though a short 50 °C H_2O purge cycle occurred during both seasons, the fact that a seasonal partitioning difference still appeared suggests that the partitioning is not quickly reversible from the particulate organic phase as collected and analyzed by TAG.

Fig. 3*B* focuses on oxygenated species only, whereas Fig. 3*C* shows compounds with no oxygen content, both including additional compound classes that were not in Fig. 3*A* because they do not extend the entire phase transitioning range. The nonoxygenated species follow the expected trend of molecules entering the particle phase with increased carbon number. Because n-alkanes are straight chained, and have very low polarity, they do not enter the particle phase until larger carbon numbers than all other compound classes seen here. Otherwise stated, n-alkanes have higher vapor pressures per carbon number than other compound classes observed.

Table 1. Parameters used for phase partitioning modeling.

	Retention time (minutes)	O:C ratio	Summer vap. pressure (Torr)	Fall vap. pressure (Torr)
			Beilstein database	Beilstein database
Alkanes				
Tridecane	26.17	0.00	3.56E-02	1.39E-02
Tetradecane	27.87	0.00	1.70E-02	6.14E-03
Pentadecane	29.46	0.00	5.66E-03	1.91E-03
Hexadecane	30.94	0.00	1.09E-03	3.41E-04
Heptadecane	32.34	0.00	3.30E-04	9.70E-05
Octadecane	33.67	0.00	1.17E-04	3.20E-05
Nonadecane	34.94	0.00	2.53E-05	6.42E-06
Eicosane	36.14	0.00	8.74E-06	2.07E-06
Heneicosane	37.29	0.00	3.21E-06	7.05E-07
Docosane	38.39	0.00	7.14E-07	1.45E-07
Tricosane	39.43	0.00	3.00E-07	5.69E-08
Tetracosane	40.44	0.00	8.89E-08	1.57E-08
Pentacosane	41.41	0.00	4.12E-08	6.79E-09
Hexacosane	42.35	0.00	8.28E-09	1.28E-09
Heptacosane	43.28	0.00	4.04E-09	5.88E-10
Octacosane	44.18	0.00	8.37E-10	1.12E-10
Nonacosane	45.07	0.00	2.47E-10	3.06E-11
Triacontane	45.96	0.00	6.70E-11	7.71E-12
Hentriacontane	46.87	0.00	1.55E-11	1.66E-12
Alkanoic acids				
Heptanoic acid	21.82	0.29	1.77E-02	6.23E-03
Octanoic acid	23.89	0.25	4.25E-03	1.41E-03
Nonanoic acid	25.72	0.22	1.79E-03	5.32E-04
Decanoic acid	27.42	0.20	4.26E-04	1.21E-04
Undecanoic acid	28.99	0.18	1.50E-04	4.15E-05
Dodecanoic acid	30.48	0.17	2.32E-05	6.16E-06
Tetradecanoic acid	33.17	0.14	2.43E-06	4.29E-07
Hexadecanoic acid	35.66	0.13	8.65E-07	1.88E-07
Octadecanoic acid	37.94	0.11	1.90E-07	3.77E-08
	Summer	Fall		
Avg temperature	299.3 K	289.1 K		
Avg PM	32.3 $\mu g\,m^{-3}$	42.9 $\mu g\,m^{-3}$		
Avg f_{om}	0.41	0.35		
Avg MW_{om}	200 $g\,mol^{-1}$	200 $g\,mol^{-1}$		

PM is particulate matter in the $PM_{2.5}$ size range, f_{om} is the fraction of PM composed of organic matter, and MW_{om} is the molecular weight of organic matter.

Oxygenated classes enter the particle phase at much lower carbon numbers because of their high polarity and hence have lower vapor pressures per carbon number than hydrocarbons. Interestingly, the oxygenated compound classes all "appear" to enter the particle phase again at the lowest carbon numbers. This trend could be a real observation or the result of a sampling (collection) or desorption (thermal decomposition) artifact. However, it seems only oxygenated species show this trend (Fig. 3*B* and *C*).

Specific high-volatility oxygenated organics have been suggested to enter the particle phase much more efficiently than predicted by traditional partitioning theory (23). Volkamer et al. suggest three possible mechanisms for the loss of gas-phase glyoxal to particles, including irreversible loss to particle surface area, reversible loss through partitioning to aerosol liquid water by Henry's law, or reversible loss through partitioning to total oxygenated organic material by smaller than previously predicted activity coefficients.

It may also be possible that these small oxygenated compounds are present in the particle phase not only as parent compounds, but also as thermal decomposition products of unstable peroxides (24) and/or the decomposition product of larger oligomers (25–27). Ultimately, there are several explanations that would point toward additional SOA compared to theoretical SOA production.

Comparison with Modeled Phase Partitioning

Phase partitioning of semivolatile organic compounds is traditionally represented by the gas-particle partitioning constant K_p ($m^3\,\mu g^{-1}$) and is derived as

$$K_p = \frac{F_i/\mathrm{PM}}{A_i} = \frac{f_{\mathrm{om}}760RT}{\mathrm{MW_{om}}\zeta_i p^{\circ}_{L,i}10^6}, \quad [1]$$

where F_i is the particle-phase concentration of compound i ($ng\,m^{-3}$), A_i is the gas-phase concentration of compound i ($ng\,m^{-3}$), PM is total particulate matter ($\mu g\,m^{-3}$), R is the gas constant (8.2×10^{-5} $m^3\,atm\,mol^{-1}\,K^{-1}$), 760 is a pressure conversion factor, T is ambient temperature (K), f_{om} is the fraction of total aerosol mass that is organic matter, MW_{om} is the average molecular weight of organic matter in the aerosol ($g\,mol^{-1}$), ζ_i is the activity coefficient (i.e., inversely related to a compound's affinity for the particle phase) of compound i, $p^{\circ}_{L,i}$ is the liquid (or subcooled) vapor pressure of compound i (Torr), and 10^6 is a mass conversion factor (28). Here, we are attempting to understand the K_p values for $PM_{2.5}$, and we must make the assumption that the composition measured by AMS and TAG at $PM_{1.0}$ and $PM_{1.5}$, respectively, is representative of the composition of $PM_{2.5}$.

In order to determine the fraction of a compound that is present in the particle phase, the following relationship can be applied to convert partitioning information from K_p space to fractional particle-phase space:

$$\frac{K_p \times \mathrm{PM}}{(K_p \times \mathrm{PM} + 1)} = \frac{F_i/A_i}{(F_i/A_i + 1)} = \frac{F_i}{F_i + A_i}. \quad [2]$$

We will model the alkanes and alkanoic acids because they are on opposite extremes of the phase partitioning figures (Fig. 3). Modeled phase partitioning under average ambient conditions

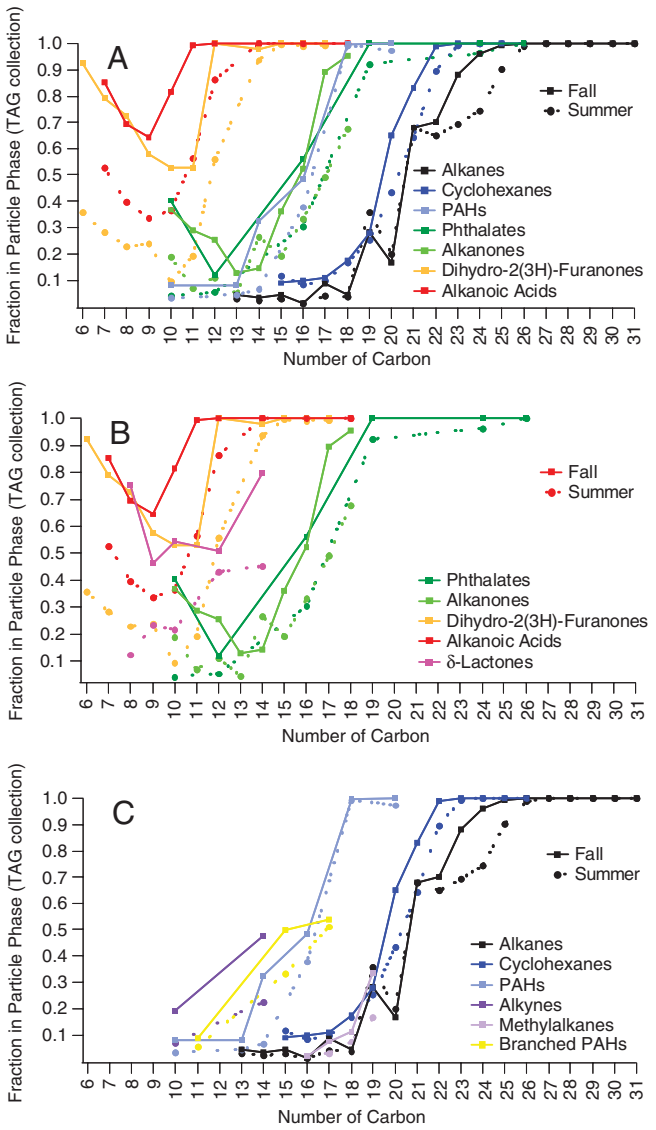

Fig. 3. Phase transitioning curves for several major compound classes as observed by TAG at Riverside, CA. (*A*) Compounds color coded by compound class and separate averages calculated by season (fall = squares, *Solid Lines*; summer = circles, *Dotted Lines*). The fraction of each compound in the particle phase is shown on the *y* axis, and the *x* axis is sorted by the number of carbon atoms in each molecule. (*B*) A separation of oxygenated molecules. (*C*) A separation of pure hydrocarbons.

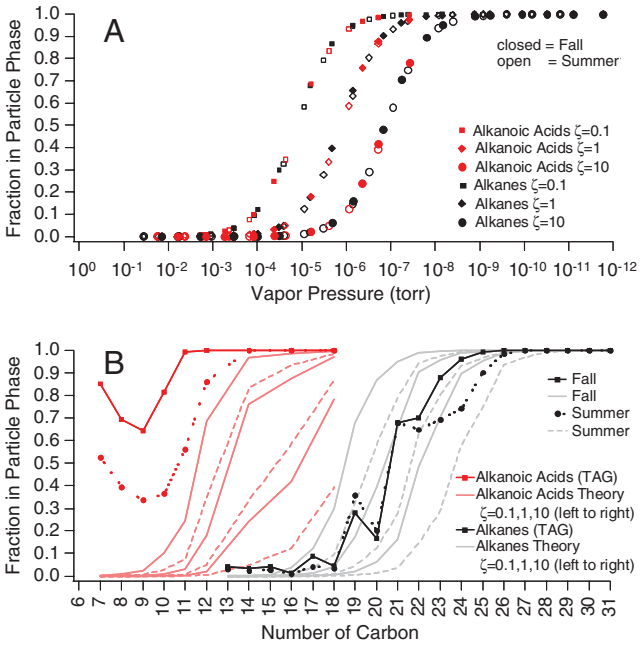

Fig. 4. Modeled phase partitioning behavior for alkanes and alkanoic acids under average conditions in Riverside, CA. (*A*) Particle-phase fraction of each compound is plotted on the *y* axis as a function of liquid vapor pressure (*x* axis). Two seasonal averages are calculated: summer (open symbols) and fall (closed symbols). Values for three separate activity coefficients (ζ) are plotted. (*B*) The same modeled values from the previous figure, now as a function of the carbon number. TAG observations of alkanoic acids and alkanes are included for comparison.

at Riverside during the summer and fall have been plotted in Fig. 4*A* as a function of compound vapor pressure for C_{13}–C_{31} alkanes and C_7–C_{18} alkanoic acids if $\zeta = 0.1$, 1, or 10. Vapor pressures ($p^{\circ}_{L,i}$) are taken from the CrossFire Beilstein Database (29) and corrected for temperature by using the Clausius–Clapeyron relationship:

$$P_2 = P_1 \times e^{\frac{\Delta H}{R}\left(\frac{1}{T_1}-\frac{1}{T_2}\right)}, \quad [3]$$

where P_2 is the desired vapor pressure (Torr), P_1 is the Beilstein vapor pressure (Torr), T_1 is the temperature for which the Beilstein vapor pressure was calculated (K), T_2 is the ambient temperature in Riverside (K), ΔH is the compound's enthalpy of vaporization (J mol^{-1}) found in the CrossFire Beilstein Database, and R is the gas constant (8.31 J mol^{-1} K^{-1}). All vapor pressures are listed in Table 1. We use a MW_{om} value of 200 g mol^{-1}, as is used in previous work (27) and is close to the average molecular weight of species observed by TAG (i.e., 220 g mol^{-1}), and PM is measured by BAM. The fraction of particulate matter composed of organic matter (f_{om}) is determined by dividing total AMS OA by the sum of all AMS species (i.e., organics, SO_4^{2-}, NO_3^-, NH_4^+, chloride) plus EC. Because EC was not measured during the fall, the same fraction of total $PM_{2.5}$ mass composed of EC during the summer (i.e., 4%) was used to calculate an approximate fall EC concentration.

Fig. 4*B* shows the same partitioning behavior plotted as a function of carbon number instead of vapor pressure. Under identical atmospheric conditions, an individual compound can shift from 5% in the particle phase to over 80% in the particle phase when modeled activity coefficients decrease from 10 to 0.1, as is seen with a C_{21} alkane and C_{14} alkanoic acid.

TAG observations of alkanes and alkanoic acids are included in Fig. 4*B* for comparison to theoretical calculations. TAG observations of alkane phase transitioning roughly fall between modeled alkane phase transitioning with activity coefficients of 1 and 10. In a previous study, the average activity coefficient calculated by using two separate models (UNIFAC and Hansen) for alkanes in three separate types of particles was found to be 6.3 ± 4.6 (30), within the range observed here. The slope of TAG-observed alkane phase transitioning appears broader than the steeper slope of the modeled alkane phase transitioning. This gradual slope is likely because of TAG's incomplete collection of the gas phase, which increases the particle-phase fraction of smaller carbon-number compounds. TAG observations of alkanoic acid phase transitioning fall below the range of modeled alkanoic acid phase transitioning. According to this comparison, TAG-observed alkanoic acid phase transitioning matches a modeled phase transition with activity coefficients less than 0.1. In the previous study (30), alkanoic acids were modeled to have an activity coefficient of 1.6 ± 1.4, a larger value than observed here. The error associated with TAG measurements of phase partitioning is dominated by incomplete gas-phase collection and at maximum

can be viewed as the difference between observations and theory. Here it is seen that, whereas alkanes approximately follow an expected phase transitioning curve, the alkanoic acids have increasingly large errors associated with smaller molecular weights. It remains uncertain whether this deviation of measurement from theory for phase partitioning of oxygenated species is actually occurring in the atmosphere, in the collection/desorption system, or as a combination of the two.

Conclusions and Discussion

The TAG system stands to offer critical high time-resolution information to the modeling efforts of OA formation and growth. TAG has been shown to capture a critical window of semivolatile organic compounds that partition between the gas and particle phases under typical atmospheric conditions and are often ignored by both gas- and particle-phase studies because of interference between physical states. By using in situ TAG measurements of both gas- and particle-phase semivolatile organic compounds, phase transitioning has been observed for several common compound classes. It has been shown that the TAG-observed phase transition for these compound classes occurs within the expected range of compound vapor pressures (10^{-2}–10^{-8} Torr), with nonpolar alkanes transitioning at larger carbon numbers relative to other classes and polar alkanoic acids transitioning at smaller carbon numbers relative to other classes.

In previous work we have explored TAG's ability to efficiently collect a particle-phase sample. Whereas TAG appears to capture the variability of semivolatile compounds' gas-phase fraction, it is apparent that the entire mass of the gas phase is not collected. TAG measurements do indicate whether a semivolatile compound is dominantly in the vapor phase, in the particle phase, or partitioning between the two phases. The transition from vapor to particle phase as a function of carbon number and compound class is observed through speciated and time-resolved TAG measurements of semivolatile organic compounds.

Phase partitioning measurements using the TAG technique can be improved upon in future studies with a more efficient gas-phase collection substrate along with the use of gas-phase calibration standards. TAG measurements of gas- and particle-phase concentrations of semivolatile organic compounds can be obtained with the high time resolution (i.e., 1 hour) that is necessary to gain a better understanding of VOC reaction pathways in the atmosphere and derive accurate partitioning parameters for ambient aerosol mixtures. These parameters are potentially one of the major missing links to correctly modeling aerosol formation and growth in the atmosphere.

Methods

Information regarding TAG design, compound quantification, and data reduction can be found in previous papers (14, 31–33). Details on TAG calibration as performed during SOAR can be found in ref. 33. Methods for mass spectral identification, chromatogram integrations, and subsequent data processing are described by Williams et al. (31). Compound vapor pressures were derived for observed temperatures from the Beilstein Data Field Reference Guide (v.4) by using the MDL CrossFire Commander (v.7) search engine (29) and from the Environmental Protection Agency database by using the MPBPWIN v1.42 engine (21).

ACKNOWLEDGMENTS. We thank Ken Docherty, Jose Jimenez, Paul Ziemann, David Snyder, Jamie Schauer, Angela Miller, and Megan McKay for their assistance during SOAR and allowing use of their data (K.D. and J.J. for AMS data, D.S. and J.S. for EC data, A.M. for VOC GC/MS data, and M.M. for PAR data). The authors also thank Jim Pankow and Chris Cappa for helpful discussions. This work was supported by the California Air Resources Board (CARB) award 03-324. We thank CARB for providing BAM data.

1. Dockery DW, et al. (1993) An association between air pollution and mortality in six U.S. cities. *N Engl J Med* 329:1753–1759.
2. Schwartz J, et al. (2001) The concentration—response relation between air pollution and daily deaths. *Environ Health Perspect* 109:1001–1006.
3. Jang M, Ghio AJ, Cao G (2006) Exposure of BEAS-2B cells to secondary organic aerosol coated on magnetic nanoparticles. *Chem Res Toxicol* 19:1044–1050.
4. Pope CA, III, Ezzati M, Dockery DW (2009) Fine-particulate air pollution and life expectancy in the United States. *N Engl J Med* 360:376–386.
5. Intergovernmental Panel on Climate Change (IPCC) (2007) *Climate Change 2007: The Physical Science Basis. Contribution of Working Group I to the Fourth Assessment Report of the Intergovernmental Panel on Climate Change* (Cambridge Univ Press, Cambridge, UK).
6. Kanakidou M, et al. (2005) Organic aerosol and global climate modelling: A review. *Atmos Chem Phys* 5:1053–1123.
7. Ramanathan V, Crutzen PJ, Kiehl JT, Rosenfeld D (2001) Atmosphere—Aerosols, climate, and the hydrological cycle. *Science* 294:2119–2124.
8. Zhang Q, et al. (2007) Ubiquity and dominance of oxygenated species in organic aerosols in anthropogenically-influenced northern hemisphere mid-latitudes. *Geophys Res Lett* 34:L13801.
9. Goldstein AH, Galbally IE (2007) Known and unexplored organic constituents in the Earth's atmosphere. *Environ Sci Technol* 41:1514–1521.
10. Heald CL, et al. (2008) Total observed organic carbon (TOOC) in the atomsphere: A synthesis of North American observations. *Atmos Chem Phys* 8:2007–2025.
11. Donahue NM, Robinson AL, Stanier CO, Pandis SN (2006) Coupled partitioning, dilution, and chemical aging of semivolatile organics. *Environ Sci Technol* 40:2635–2643.
12. Docherty KS, et al. (2008) Apportionment of primary and secondary organic aerosols in southern California during the 2005 study of organic aerosols in Riverside (SOAR-1). *Environ Sci Technol* 42:7655–7662.
13. Hallquist M, et al. (2009) The formation, properties and impact of secondary organic aerosol: Current and emerging issues. *Atmos Chem Phys* 9:5155–5236.
14. Williams BJ, Goldstein AH, Kreisberg NM, Hering SV (2006) An in-situ instrument for speciated organic composition of atmospheric aerosols: Thermal desorption aerosol GC/MS-FID (TAG). *Aerosol Sci Tech* 40:627–638.
15. Canagaratna MR, et al. (2007) Chemical and microphysical characterization of ambient aerosols with the aerodyne aerosol mass spectrometer. *Mass Spectrom Rev* 26:185–222.
16. Snyder DC, Schauer JJ (2007) An inter-comparison of two black carbon aerosol instruments and a semi-continuous elemental carbon instrument in the rrban environment. *Aerosol Sci Tech* 41:463–474.
17. Gentner DR, Harley RA, Miller AM, Goldstein AH (2009) Diurnal and seasonal variability of gasoline-related volatile organic compound emissions in Riverside, California. *Environ Sci Technol* 43:4247–4252.
18. Docherty KS, Ziemann PJ (2001) On-line, inlet-based trimethylsilyl derivatization for gas chromatography of mono- and dicarboxylic acids. *J Chromatogr A* 921:265–275.
19. Wang L, Atkinson R, Arey J (2007) Dicarbonyl products of the OH radical-initiated reactions of naphthalene and the C1- and C2-alkylnaphthalenes. *Environ Sci Technol* 41:2803–2810.
20. Fine PM, Chakrabarti B, Krudysz M, Schauer JJ, Sioutas C (2004) Diurnal variations of individual organic compound constituents of ultrafine and accumulation mode particulate matter in the Los Angeles basin. *Environ Sci Technol* 38:1296–1304.
21. EPA MPBPWIN (2008). v1.42. http://epa.gov/oppt/exposure/pubs/episuite.htm.
22. Eiguren-Fernandez A, Miguel AH, Froines JR, Thurairatnam S, Avol EL (2004) Seasonal and spatial variation of polycyclic aromatic hydrocarbons in vapor-phase and $PM_{2.5}$ in southern California urban and rural communities. *Aerosol Sci Tech* 38:447–455.
23. Volkamer R, et al. (2007) A missing sink for gas-phase glyoxal in Mexico City: Formation of secondary organic aerosol. *Geophys Res Lett* 34:L19807.
24. Tobias HJ, Docherty KS, Beving DE, Ziemann PJ (2000) Effect of relative humidity on the chemical composition of secondary organic aerosol formed from reactions of 1-tetradecene and O_3. *Environ Sci Technol* 34:2116–2125.
25. Jang M, Carroll B, Chandramouli B, Kamens R (2003) Particle growth and acid-catalyzed heterogeneous reactions of organic carbonyls on preexisting aerosols. *Environ Sci Technol* 37:3828–3837.
26. Jang M, Czoschke NM, Lee S, Kamens RM (2002) Heterogeneous atmospheric aerosol production by acid-catalyzed particle-phase reactions. *Science* 298:814–817.
27. Barsanti KC, Pankow JF (2004) Thermodynamics of the formation of atmospheric organic particlulate matter by accretion reactions—Part 1: Aldehydes and ketones. *Atmos Environ* 38:4371–4382.
28. Pankow JF (1994) An absorption model of gas/particle partitioning of organic compounds in the atmosphere. *Atmos Environ* 28:185–188.
29. CrossFire Beilstein Database (2008) Database BS080100AB with 10322966 compounds. Elsevier Information Systems.
30. Chandramouli B, Jang M, Kamens RM (2003) Gas-particle partitioning of semi-volatile organics on organic aerosols using a predictive activity coefficient model: analysis of the effects of parameter choices on model performance. *Atmos Environ* 37:853–864.
31. Williams BJ, et al. (2007) Chemical speciation of organic aerosol during the international consortium for atmospheric research on transport and transformation 2004: results from in situ measurements. *J Geophys Res* 112:D10S26.
32. Goldstein AH, et al. (2008) Thermal desorption comprehensive two-dimensional gas chromatography for in-situ measurements of organic aerosols. *J Chromatogr A* 1186:340–347.
33. Kreisberg NM, Hering SV, Williams BJ, Worton DR, Goldstein AH (2009) Quantitation of hourly speciated organic compounds in atmospheric aerosols, measured by in-situ thermal desorption aerosol gas chromatography (TAG). *Aerosol Sci Tech* 43:38–52.